

Effects of Humidity on the Electrical Behaviour of $\text{Sr}_{0.97}\text{Ti}_{0.97}\text{Fe}_{0.03}\text{O}_{3-\delta}$

M. E. V. Costa,^a J. R. Jurado,^b M. T. Colomer^b and J. R. Frade,^{a*}

^aCeramics and Glass Engineering Department, University of Aveiro, 3810 Aveiro, Portugal

^bInstitute of Ceramics and Glasses, CSIC, 28500 Arganda del Rey, Madrid, Spain

Abstract

It is widely recognised that the electrical behaviour of acceptor-doped strontium titanate ceramics is often controlled by resistive grain boundaries. This work shows that the electrical behaviour of $\text{Sr}_{0.97}\text{Ti}_{1-x}\text{Fe}_x\text{O}_{3-\delta}$ materials may also be affected by other factors such as the humidity in the atmosphere, especially for materials with open porosity. For example, the impedance of dense samples with large grain size may exceed the impedance of samples with residual porosity. The bulk and grain boundary resistivities both increase with the humidity in the atmosphere. © 1999 Elsevier Science Limited. All rights reserved

Keywords: grain boundaries, impedance, titanates, sensors.

1 Introduction

Waser and co-authors proposed a defect chemistry model for the resistive grain boundaries of acceptor doped strontium titanate.^{1–3} The transient behaviour is suitable to distinguish the conductivity of grain boundaries from the true bulk transport because the corresponding relaxation times usually differ by about three orders of magnitude. Impedance spectroscopy in a typical frequency range 1 Hz to 10 MHz is thus also suitable to investigate the bulk and grain boundary transport properties, and the effects of interfacial processes, as reported for other materials.^{4–7} This technique may also be used to investigate the effects of working conditions (e.g. temperature and composition of the atmosphere).

Work performed with single crystals showed that the bulk conductivity tends to become mainly ionic in air (or moderately oxidising conditions), at least for temperatures lower than about 500°C.^{8,9} The grain boundary conductivity may be mainly p-type

in identical conditions, and the model behaviour proposed by Waser and co-authors¹ predicted a V-type grain boundary conductivity profile at sufficiently low temperatures. This model assumes that segregation of donor states is responsible for depleting the concentration of positively charged carriers ($h\cdot$ and $V_{O^{\cdot\cdot}}$). Those authors also proposed a W-type profile (due to $p \rightarrow n$ inversion) at sufficiently high temperatures, with an activation energy $E_{\sigma_{gb}} \approx W_g/2 \approx 1.6eV$, where W_g is the band gap.

2 Experimental Procedure

Powders of $\text{Sr}_{0.97}\text{Ti}_{0.97}\text{Fe}_{0.03}\text{O}_{3-\delta}$ were prepared by solid state reactions from strontium carbonate, and titanium and iron oxides, by calcination at 1100°C, for 12 h. These powders were then milled to destroy agglomerates, and to obtain uniaxially pressed disks, which were sintered at 1500°C for 20 h (sample A), or at 1450°C for 4 h (sample B). The Archimedes method was used to evaluate the density. Sample A was about 94% dense (probably without open porosity), and sample B was about 92% dense. These samples were monophasic, within the detection limits of X-Ray diffraction.

The HP Impedance Analyzer (HP1492A) with a frequency range 10Hz–10MHz was used to obtain impedance spectra in air. A suitable paste was used to paint Pt electrodes, and these were fired at 900°C. Alternative Au electrodes were sputtered on sample B. The complex impedance spectra of these materials usually comprise two or three well defined arcs (as illustrated in Fig. 1). Impedance spectra were also obtained in air with adjusted humidity using a Solartron 1260 impedance bridge. The humidity was measured by a commercial sensor (Testoterm 6010).

3 Bulk and Grain Boundary Conductivities in Air

Figure 1 shows typical impedance spectra for sample A, with Pt electrodes, and sample B with either

*To whom correspondence should be addressed. Fax: +34-351-34-25300; e-mail: jfrade@cv.ua.pt

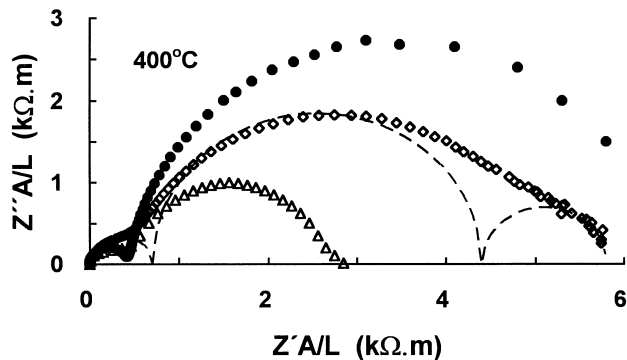


Fig. 1. Impedance spectra obtained for sample A with Pt electrodes (closed circles), and for sample B with Pt electrodes (open circles), or Au electrodes (open triangles), at 400°C.

Pt or Au electrodes, at 400°C. These measurements were performed in air, and without control of the atmospheric humidity. Spectra obtained at other temperatures also show a small (but clearly defined) arc at high frequencies, a large arc in the intermediate frequency range, and sometimes a third component at still lower frequencies, especially for sample B with Pt electrodes. An attempted fitting for the different contributions of this spectrum is thus shown dashed in Fig. 1. Peak frequencies of the high and intermediate frequency arcs are shown in Fig. 2. At relatively low temperatures ($T < 300^\circ\text{C}$) the intermediate and low frequency arcs cannot be evaluated with the actual frequency range (10 Hz–10 MHz).

At 400°C the intermediate and high peak frequencies are about 10^2 Hz and 10^5 Hz, respectively. These frequencies are within the ranges of the grain boundary and bulk contributions reported for

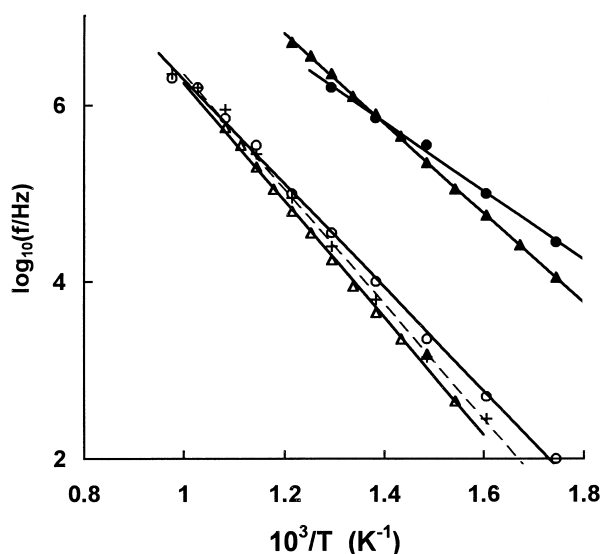


Fig. 2. Peak relaxation frequencies for sample A with Pt electrodes (triangles), sample B with Au electrodes (circles), and sample B with Pt electrodes (+). The closed symbols denote the high frequency terms ($\rho_{hf} = R_{hf}A/L$), and the open symbols and (+) represent the intermediate frequency terms.

acceptor doped strontium titanate.^{1,2} The corresponding resistivity values $\rho_{hf} = R_{hf}A/L$, (where A is the electrode area, and L the thickness of the sample), should thus correspond to the bulk resistivity and are shown in Fig. 3. The intermediate frequency component $\rho_{if} = R_{if}A/L$ is probably at least one order of magnitude lower than the true grain boundary resistivity because the grain boundaries across the sample represent a small fraction of the sample thickness.

The activation energy of the high frequency resistivity of sample A ($\approx 0.98\text{eV}$) is relatively close to a typical value reported for acceptor doped strontium titanate, and the activation energy for the intermediate frequency term ($\approx 1.34\text{eV}$) is intermediate between the values for the V-type ($\approx 1\text{eV}$) and W-type ($\approx 1.6\text{eV}$) profiles proposed by Waser and coauthors.² In addition, the $\log(\rho_{hf})$ versus $1/T$ plot obtained for sample A suggests an increase in activation energy with increasing temperature. The increase in activation energy may indicate a change from the V-type to the W-type profile, as proposed by Waser and co-authors.²

On using Pt electrodes one obtains similar values of high frequency resistivities for samples A and B (Fig. 3). However, the differences in the intermediate frequency term (presumably due to resistive grain boundaries) are somewhat surprising because the average grain size of sample A is larger than for sample B. Sample B thus contains a greater number of grain boundaries per unit thickness, and the values of ρ_{if} should be higher for sample B than for sample A. The peak relaxation frequencies are displaced to slightly higher values (Fig. 2).

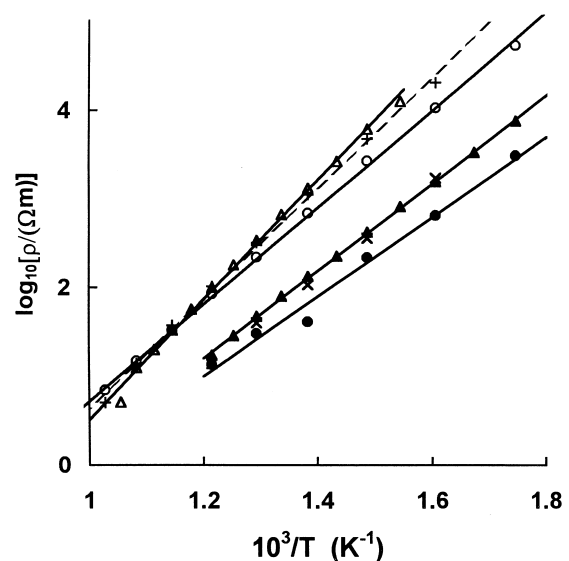


Fig. 3. Equivalent resistivities obtained for sample A with Pt electrodes (triangles), sample B with Au electrodes (circles), and sample B with Pt electrodes (+). The closed symbols denote the high frequency terms ($\rho_{hf} = R_{hf}A/L$). The open symbols and (+) represent the intermediate frequency terms ($\rho_{if} = R_{if}A/L$).

The activation energies are also somewhat lower for sample B than for sample A. The activation energy of ρ_{if} is 1.32 eV for sample A with Pt electrodes, 1.24 eV for sample B with Pt electrodes, and 1.09 eV for sample B with Au electrodes. The activation energies of ρ_{hf} are 0.93 eV for sample A with Pt electrodes, and 0.77 eV for sample B with Au electrodes.

In order to be able to interpret the differences between samples A and B one may consider the differences in firing temperature and time. In fact, the concentrations of ionic defects (e.g. $[V_{Sr}^{''}]$, $[V_{O}^{\cdot}]$, $[Fe_{Ti}^{\cdot}]$) may decrease on cooling,^{10,11} and this is expected to affect the transport properties. For example, a lower concentration of Fe_{Ti}^{\cdot} may prevent the trapping effect exerted on electron holes.¹¹

The greatest differences between results shown in Figs 2 and 3 were obtained on changing from Pt to Au electrodes; this includes differences in peak frequencies, and activation energies. These observations raise doubts about the true nature of the intermediate frequency arc because the grain boundary conductivity should be independent of the electrodes. One should thus consider unexpected differences in working conditions. For example, additional results (in Section 4) demonstrate that humidity may play a very significant role. Unfortunately the experiments reported in Figs 1–3 were performed without control of the atmospheric humidity.

4 Effects of Atmospheric Humidity

Figure 4 shows that resistivity measurements increase with the atmospheric humidity. These effects are exerted in two different frequency ranges, which can be related to the peak frequency ranges shown in Fig. 2. One may thus conclude that the atmospheric humidity affects both the high and intermediate frequency processes. Results obtained at significantly lower temperatures (200°C) and in the frequency range 1 Hz to 1 MHz only show the high frequency contribution (Fig. 5). In addition, the relative effects of humidity tend to decrease with decreasing temperature, within the range of actual working conditions (200 to 400°C).

Comparison of results for 200°C and 400°C shows that the relative effects of humidity on the high frequency process tend to increase with temperature. The temperature dependence of the high frequency resistivity measurements (ρ_{hf}) is thus probably stronger in dry conditions than in wet atmospheres. This is more likely to occur for sample B (with residual porosity) than for dense sample A,

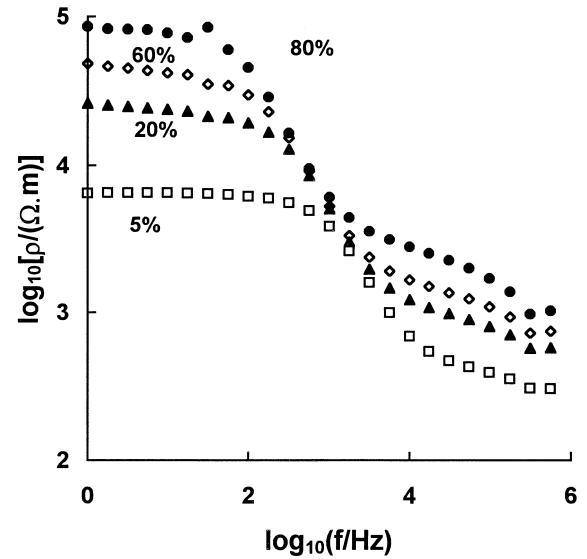


Fig. 4. Resistivity of sample B with Au electrodes as a function of humidity, at 400°C. The values of relative humidity are also shown.

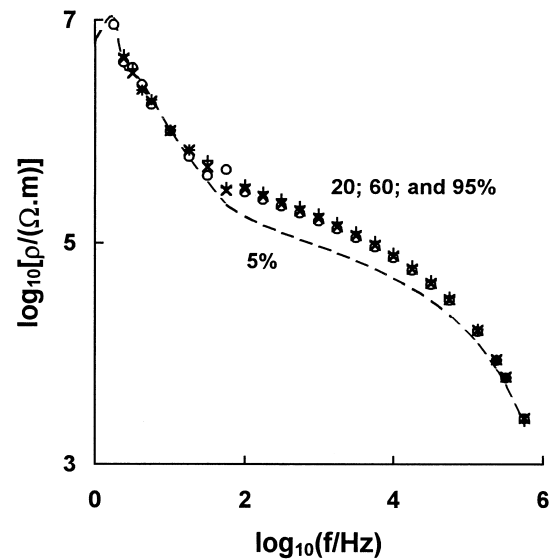


Fig. 5. Resistivity of sample B with Au electrodes as a function of humidity, at 200°C. The results obtained for 20% (o), 60% (x) and 95% humidity (+) are similar.

because the absence of open porosity may prevent the effects of humidity on dense samples; this may explain the differences in activation energy for samples A and B. A similar effect may explain the differences in activation energy for the intermediate frequency component.

The intermediate peak frequency corresponds to the inflection point shown by the $\log(\rho)$ versus $\log(f)$ plots. Figure 4 thus shows that the intermediate peak frequency varies with the humidity. This may also explain differences between the peak frequencies obtained for sample B (clearly affected by humidity), and the corresponding results for sample A (presumably much less dependent on the humidity).

5 Conclusions

This work shows that one should be cautious about the electrical characterisation of bulk and grain boundary conductivities of this type of strontium titanate based materials because humidity may play a very significant role. For example, a change from 5% to 95% humidity may cause increase in resistivity by about one order of magnitude at 400°C. These changes occur in two separate frequency ranges which correspond to the expected ranges for the bulk and grain boundary processes.

The type of results reported in this work may be used to select suitable frequency ranges for potential sensor applications. However, further work is needed to assess the selectivity and other features of these potential devices. A suitable design of porosity and other microstructural features might also be needed to enhance the sensitivity, minimise the response time, and/or the long term drift, etc.

Acknowledgements

This work was sponsored by the Portuguese Foundation for Science and Technology, and Program PRAXIS XXI, under Contract PRAXIS XXI/3/3.1/MMA/1760/95, and in the form of a grant BCC/4273/94.

References

1. Volmann, M. and Waser, R., Grain boundary defect chemistry of acceptor-doped titanates: Space charge layer width. *J. Amer. Ceram. Soc.*, 1994, **77**, 235–243.
2. Volmann, M., Hagenbeck, R. and Waser, R., Grain boundary defect chemistry of acceptor-doped titanates: Inversion layer and low field conduction. *J. Amer. Ceram. Soc.*, 1997, **80**, 2301–2314.
3. Volmann, M. and Waser, R., Grain boundary defect chemistry of acceptor-doped titanates: High field effects. *Journal of Electroceramics*, 1997, **1**, 51–64.
4. Bauerle, J. E. and Hriko, J., Interpretation of the resistivity temperature dependence of high purity $(\text{ZrO}_2)_{0.9}(\text{Y}_2\text{O}_3)_{0.1}$. *J. Phys. Chem. Solids*, 1969, **30**, 565–570.
5. Bauerle, J. E., Study of solid electrolyte polarization by a complex admittance method. *J. Phys. Chem. Solids*, 1969, **30**, 2657–2670.
6. Kleitz, M. and Kennedy, J. H. Resolution of multi-component impedance diagram. In *Fast Ion Transport in Solids*, ed. Vashishta, P., Mundy, J. N. and Shenoy, G. R. Elsevier, 1979, pp. 185–188.
7. Rodrigues, C. M. S. Labrincha and J. A. Marques, F. M. B., Study of YSZ-glass composites by impedance spectroscopy. *J. Electrochem. Soc.*, 1997, **144**, 4303–4309.
8. Waser, R., Bulk conductivity and defect chemistry of acceptor doped strontium titanate in the quenched state. *J. Amer. Ceram. Soc.*, 1991, **74**, 1934–1940.
9. Denk, I., Munch, W. and Maier, J., Partial conductivities in SrTiO_3 : Bulk polarization experiments, oxygen concentration cell measurements, and defect chemical modelling. *J. Amer. Ceram. Soc.*, 1995, **78**, 3265–3272.
10. Moos, R. and Hardtl, K. H., Dependence of the intrinsic conductivity minimum of SrTiO_3 ceramics on the sintering atmosphere. *J. Amer. Ceram. Soc.*, 1995, **78**, 2569–2571.
11. Bieger, T., Maier, J. and Waser, R., Kinetics of oxygen incorporation in SrTiO_3 (Fe-doped): an optical investigation. *Sensors and Actuators B*, 1992, **7**, 763–768.